Electronic Properties of New Organic Conductors Based on 2,7-Bis(methylthio)-1,6-dithiapyrene (MTDTPY) with TCNQ and *p*-Benzoquinone Derivatives

Kenichi IMAEDA,* Toshiaki ENOKI,† Takehiko MORI, Hiroo INOKUCHI, Mitsuru SASAKI,††
Kazuhiro NAKASUJI,†† and Ichiro MURATA††
Institute for Molecular Science, Okazaki 444
††Department of Chemistry, Faculty of Science, Osaka University, Toyonaka, Osaka 560
(Received August 8, 1988)

The electronic properties of charge-transfer (CT) complexes based on a new organic donor MTDTPY with TCNQ and *p*-benzoquinone derivatives (fluoranil (FLL), chloranil (CHL), bromanil (BRL), and DDQ) have been investigated by means of electrical conductivity, thermoelectric power, ESR, and band calculation. β-MTDTPY-TCNQ, MTDTPY-CHL, and MTDTPY-BRL show a metallic electrical conduction. MTDTPY-CHL and MTDTPY-BRL are the first organic metals among the CT complexes with *p*-benzoquinone derivatives. The metal-insulator (M-I) transition takes place around 110, 240, and 125 K for β-MTDTPY-TCNQ, MTDTPY-CHL, and MTDTPY-BRL, respectively. The sharp ESR linewidth and large anisotropy of the transfer integral for β-MTDTPY-TCNQ and MTDTPY-CHL suggest a one-dimensional electronic property. Thus, the M-I transition for these complexes is considered to be caused by a Peierls instability. MTDTPY-CHL undergoes a first-order phase transition in the semiconducting phase. This phase transition disappears by applying pressure.

The findings of metallic conductivity in TTF-TCNQ and superconductivity in $(TMTSF)_2PF_6$ have attracted the interest of many chemists and physicists dealing with organic conductors. These new phenomena have mainly been discovered in charge-transfer (CT) complexes based on TTF and its derivative donors. It is required to explore a new class of donors for the purpose of extending the range of research for organic conductors. It is well known that polycyclic aromatic hydrocarbons form CT complexes with various acceptors. Among them, a perylene-bromine complex is famous for the first organic semiconductor with a high conductivity of $\rho_{RT}\approx 1\ \Omega$cm.[1] Thereafter, metallic conductivities down to 200 K have been observed in perylene-X (X=PF_6 and AsF_6) crystals obtained using an electrochemical technique.[2]

For the development of a new class of donors based on polycyclic aromatic hydrocarbons, we intended to introduce sulfur atoms in perylene and pyrene skeletons in order to increase the polarizability and decrease the ionization potential. 3,10-Dithiaperylene (DTPR) and 1,6-dithiapyrene (DTPY) were synthesized on the basis of such a molecular design. Most of their CT complexes were semiconductors, despite relatively high conductivities.[3] Bechgaard et al. prepared a single crystal of DTPY-TCNQ and found metallic conductivity down to 4 K.[4,5] In order to enhance the dimensionality through interchain interactions, we synthesized 2,7-bis(methylthio)-1,6-dithiapyrene (MTDTPY) substituted with two methylthio groups to DTPY. The molecular structure of MTDTPY is illustrated in Fig. 1. We reported on the synthesis and gave a brief of the physical properties of MTDTPY and their CT complexes in a previous paper,[6] which

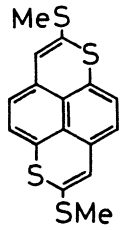

Fig. 1. Molecular structure of MTDTPY.

presents the metallic conductivities of MTDTPY complexes with TCNQ, chloranil (CHL), and bromanil (BRL). In this paper, we present the experimental results of electrical conductivity, thermoelectric power, ESR, and band calculation for MTDTPY complexes with TCNQ, fluoranil (FLL), CHL, BRL, and 2,3-dichloro-5,6-dicyano-*p*-benzoquinone (DDQ) and discuss the electronic structures in relation to their dimensionalities. The difference in electronic properties between DTPY-TCNQ and MTDTPY-TCNQ is also discussed.

Experimental

Single crystals of MTDTPY with TCNQ were prepared by a diffusion method in a CH_3CN solution. Two kinds of black needle crystals were obtained as lustrous crystal and lusterless crystal. X-Ray studies have shown that each crystal phase has a different crystal structure, where the former (α-form) is monoclinic and the latter (β-form) is triclinic.[6] The black needle crystals of MTDTPY complexes with FLL, CHL, and BRL were prepared by a slow concentration of the mixed solutions of the donor and the acceptor in CH_2Cl_2. MTDTPY-DDQ was obtained as black needle crystal by a diffusion method in a C_6H_5CN solution. All the complexes were shown to have a composition of 1 : 1 from elemental analyses. The electrical conductivity for all complexes along the long crystal axis, which corresponds to the stacking axis for β-MTDTPY-TCNQ and MTDTPY-CHL, was meas-

† Present address: Department of Chemistry, Faculty of Science, Tokyo Institute of Technology, Ookayama, Meguro-ku, Tokyo 152.

ured by a two-probe method for α-MTDTPY-TCNQ and a four-probe method for the other complexes using gold paste as electrical contacts. The conductivity under pressure up to 10 kbar for MTDTPY-CHL was carried out by means of a BeCu clamp cell with a manganin pressure sensor using Idemitsu Daphne oil #7373 as a pressure fluid medium. The thermoelectric power for β-MTDTPY-TCNQ and MTDTPY-CHL along the long crystal axis was measured by the Chaikin and Kwak method.[7] An ESR measurement was performed using a conventional X-band spectrometer Varian E112 equipped with a continuous-flow helium cryostat Oxford ESR9. A static magnetic field was applied perpendicular to the long axis of the crystals with dimensions of about 1×0.1×0.03 mm^3 for β-MTDTPY-TCNQ and about 2×0.2×0.03 mm^3 for MTDTPY-CHL. The absolute value of the spin susceptibility was determined with DPPH as a reference. Molecular orbital calculations for β-MTDTPY-TCNQ and MTDTPY-CHL were performed by the extended Hückel method.[8,9] The intermolecular overlap integral was calculated between the conduction molecular orbitals which correspond to the highest occupied molecular orbital (HOMO) for a donor and the lowest unoccupied molecular orbital (LUMO) for an acceptor. The energy band structure was obtained using the tight-binding approximation.

Results

MTDTPY-TCNQ. α-MTDTPY-TCNQ shows a simple semiconductive behavior with a resistivity at room temperature ρ_{RT} of 2.7×10^5 Ω cm and an activation energy E_a of 0.26 eV. This result can be easily understood in terms of a mixed stack structure by an X-ray diffraction study and a small degree of charge transfer of 0.3—0.4 estimated by IR and X-ray procedures.[6] On the contrary, β-MTDTPY-TCNQ with a segregated stack structure and a partial CT of 0.6—0.7[6] shows a metallic conduction with $\rho_{RT}=9.5\times10^{-3}$ Ω cm (Fig. 2). The resistivity gradually decreases down to 275 K, where it shows a broad minimum. Below 150 K, the resistivity increases steeply with an inflection in the slope around 110 K. The activation energy below 90 K is estimated to be 0.056 eV. The temperature dependence of the thermoelectric power S for β-MTDTPY-TCNQ is also shown in Fig. 2. S is almost constant down to 200 K with a negative value of −8.5 μV K^{-1} at room temperature, and it then gradually increases. Its sign changes to a positive side around 150 K. Then, S shows a maximum at 110 K and decreases rapidly.

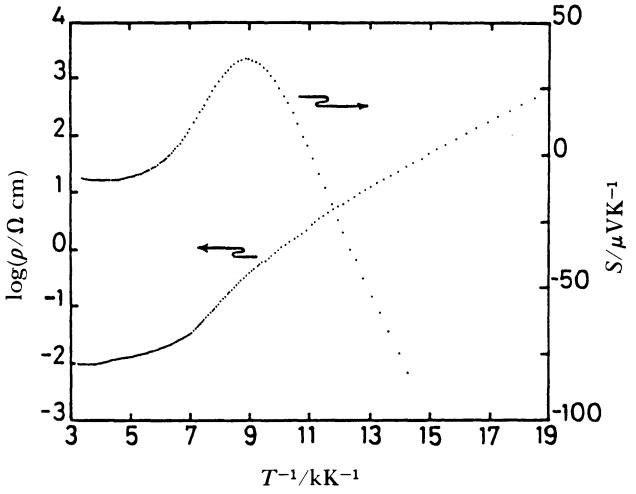

Fig. 2 .Temperature dependence of the resistivity and the thermoelectric power for β-MTDTPY-TCNQ.

β-MTDTPY-TCNQ shows a sharp ESR spectrum with a Lorentzian line shape with a g-value of 2.0024 and a linewidth of 0.87 G (1G=10^{-4} T) at room temperature. The g-value is independent of the temperature down to 110 K (Fig. 3). The ESR spectra split into two components below 110 K. The g-value of one component remains unchanged down to 50 K, around the g-value of the spectra above 110 K, while that of the other component gradually increases to 2.0034 at 50 K. Below 50 K, the two signal components approach each other. The signal with a smaller g-value is assigned to electron spins on TCNQ molecules, since its value is very close to 2.0025 of the reported value for $TCNQ^-$ anion in the LiTCNQ salt.[10] The signal with a larger g-value is assigned to electron spins on MTDTPY molecules, since the large g-shift ($\delta g=g-g_0$, g_0: g-value for free electron spin) is caused by a large spin-orbit coupling due to sulfur atoms in an MTDTPY molecule. The temperature dependence of the linewidth is also shown in Fig. 3. The linewidth decreases linearly with decreasing temperature in the metallic region. Below 110 K at the biginning of the splitting in the

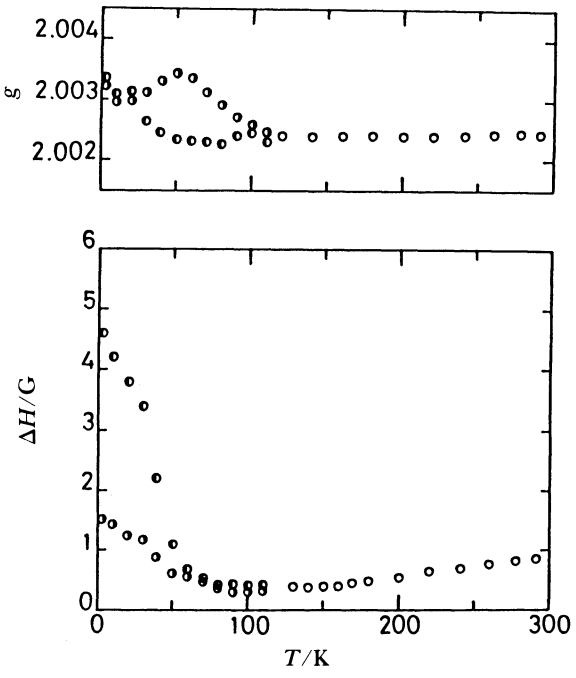

Fig. 3. Temperature dependence of the g-value and the linewidth (ΔH) in ESR spectra for β-MTDTPY-TCNQ. The half-open circles indicate the g-value and the linewidth of two components of the ESR spectra deconvoluted by a computer simulation (◑: MTDTPY, ◐: TCNQ).

spectra, the linewidths for two signal components increase with lowering temperature. The signal for TCNQ chains becomes broader than that for MTDTPY chains, where 4.5 G for the former signal and 1.5 G for the latter signal at 3 K. Figure 4 shows the temperature dependence of the spin susceptibility χ_s for β-MTDTPY-TCNQ. χ_s gradually decreases in the metallic region and then decreases steeply below 150 K. Below 110 K, it decreases exponentially and has a Curie tail due to lattice irregularities below 50 K. The estimated concentrations of localized spins are about 0.04 and 0.07% for MTDTPY and TCNQ molecules, respectively.

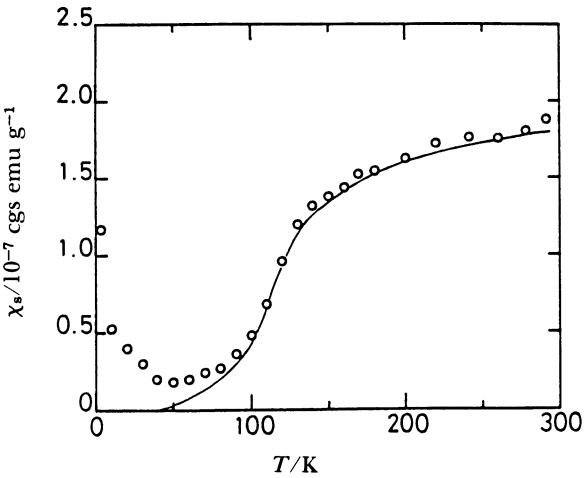

Fig. 4. Temperature dependence of the spin susceptibility (χ_s) for β-MTDTPY-TCNQ. The solid line is obtained after a subtraction of the Curie tail at low-temperatures.

Figure 5 shows the charge distribution of the HOMO in an MTDTPY molecule. The charge density on the inner sulfur atom is ten times as large as that on the outer sulfur atom. Table 1 summarizes the calculated intermolecular overlap integrals for the HOMO of MTDTPY, the LUMO of TCNQ, and the HOMO-LUMO between MTDTPY and TCNQ in β-MTDTPY-TCNQ. Both MTDTPY and TCNQ molecules have the largest overlap integrals along the stacking direction parallel to the c-axis. The ratio ($t_{\parallel}/t_{\perp}$) between intrachain and interchain transfer integrals is 24 and 44 for MTDTPY and TCNQ columns, respectively. According to IR and X-ray studies, β-MTDTPY-TCNQ has a degree of charge-transfer of 0.6—0.7.[6] The energy band structure under the degree of CT of 0.6 is shown in Fig. 6. The upper energy band corresponds to TCNQ, while the lower one corresponds to MTDTPY. Both MTDTPY and TCNQ sheets display completely one-dimensional band structures having an energy dispersion only along the stacking axis and almost flat Fermi surface.

MTDTPY-*p*-Bbenzoquinone Derivatives. MTDTPY-

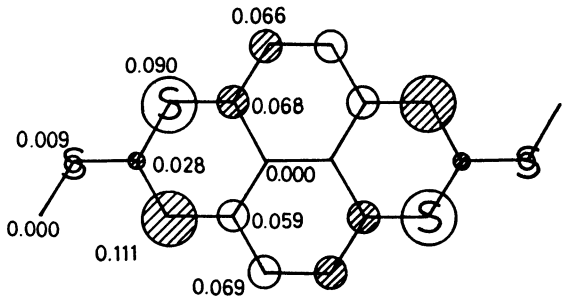

Fig. 5. Charge distribution of the HOMO for MTDTPY.

Table 1. Overlap Integrals of the HOMO, the LUMO, and the HOMO-LUMO in β-MTDTPY-TCNQ

Molecules	Crystal direction[a)]	Overlap integral $\times 10^{-3}$
MTDTPY-MTDTPY	c	11.11
MTDTPY-MTDTPY	a−c	0.46
MTDTPY-MTDTPY	a	−0.10
TCNQ-TCNQ	c	6.96
TCNQ-TCNQ	a+c	0.16
TCNQ-TCNQ	a	−0.07
MTDTPY-TCNQ	a/2+b/2+c/2	0.22

a) The definition of the crystal axes is described in Ref. 6.

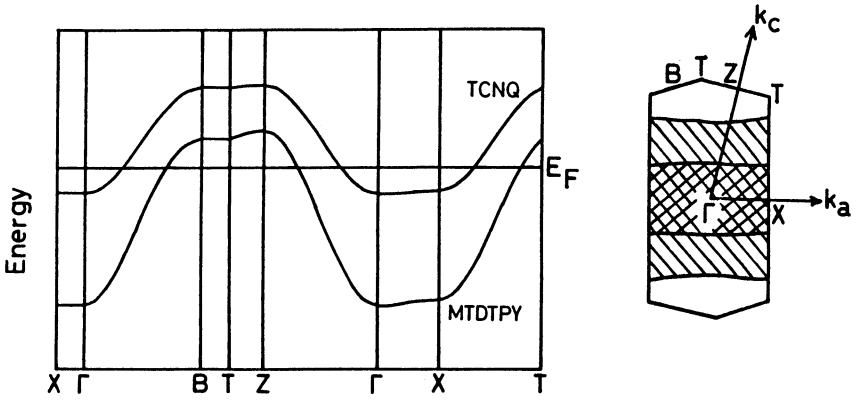

Fig. 6. Energy band structure and Fermi surface of β-MTDTPY-TCNQ. The regions shaded with // slashes and \\ slashes indicate the electron-like parts for MTDTPY and TCNQ, respectively.

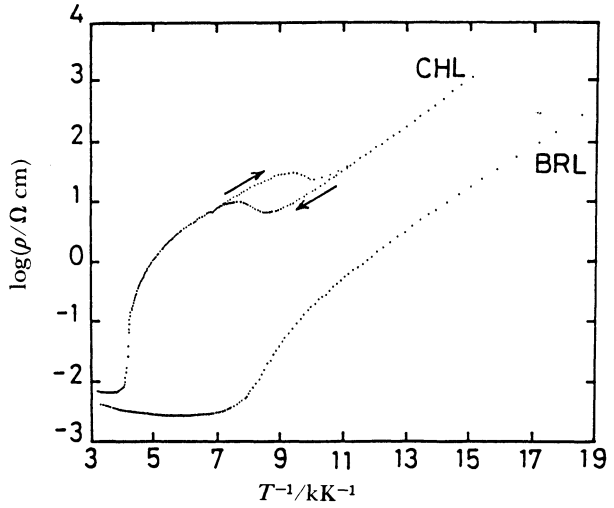

Fig. 7. Temperature dependence of the resistivities for MTDTPY-chloranil (CHL) and MTDTPY-bromanil (BRL). The arrows indicate the cooling and heating runs.

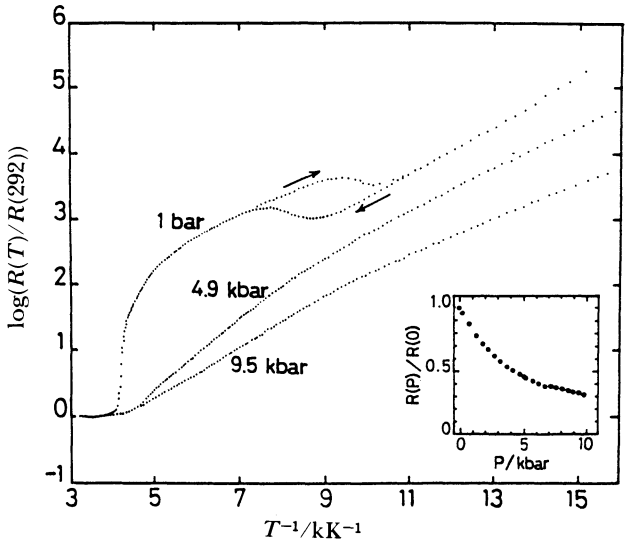

Fig. 8. Temperature dependence of the resistivities under 1 bar, 4.9 kbar, and 9.5 kbar for MTDTPY-chloranil. The inset shows the pressure dependence of the resistance at room temperature.

FLL shows a simple semiconductive behavior with E_a=0.13 eV in spite of fairly low resistivity with $\rho_{RT}=5.5\times10^{-2}$ Ω cm. MTDTPY-DDQ is also a semiconductor with ρ_{RT}=5.4 Ω cm and E_a=0.14 eV. On the other hand, MTDTPY-CHL shows a metallic conduction with $\rho_{RT}=7.0\times10^{-3}$ Ω cm (Fig. 7). The resistivity slowly decreases down to 280 K, where it shows a broad minimum. Then, the resistivity suddenly increases at 240 K. A hysteresis of the resistivity is observed around 110 K. The results of the resistivity under pressure for MTDTPY-CHL are shown in Fig. 8. The pressure dependence of the resistance at room temperature is shown in the inset. The resistance decreases monotonously with increasing pressure and the resistance at about 10 kbar becomes about one-third of that at 1 bar. Under 4.9 kbar, the metal-insulator transition temperature (T_{MI}) is lowered to 220 K compared with 240 K under 1 bar. What is noticeable is that the hysteresis of the resistivity disappears above this pressure. The activation energy E_a is 0.10 eV just below the M-I transition under 4.9 kbar. When the pressure increases to 9.5 kbar, T_{MI} is unchanged and E_a just below the M-I transition decreases to 0.078 eV due to a reduction of the band gap by pressure.

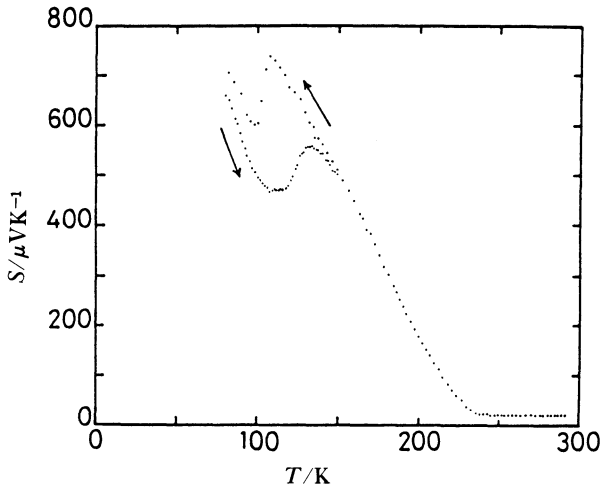

Fig. 9. Temperature dependence of the thermoelectric power for MTDTPY-chloranil. The arrows indicate the cooling and heating runs.

Figure 9 shows the temperature dependence of the thermoelectric power S for MTDTPY-CHL. S is steadily constant down to 240 K and then increases steeply. The hysteresis in the thermoelectric power is observed around the same temperature as that in the resistivity.

MTDTPY-CHL shows an ESR spectrum with a Lorentzian line shape with a g-value of 2.0059 and a linewidth of 2.2 G at room temperature. The splitting of the ESR spectra was not observed over the entire temperature region, unlike β-MTDTPY-TCNQ. The g-value is entirely independent of the temperature. Figure 10 shows the temperature dependence of the linewidth ΔH and the spin susceptibility χ_s for MTDTPY-CHL. ΔH gradually decreases down to about 120 K and then increases to 2.9 G at 3 K. χ_s gradually decreases down to 240 K, and below this temperature it decreases exponentially. Below 80 K, χ_s shows a Curie tail due to lattice irregularities in the crystal. The concentration of localized spins is about 0.03%.

Table 2 summarizes the intermolecular overlap integrals for MTDTPY-CHL. The overlap integrals along the stacking axis are largest for both donor and acceptor columns. $t_{\parallel}/t_{\perp}$ is 7 and 45 for MTDTPY and CHL columns, respectively. The degree of CT of MTDTPY-CHL has not been determined precisely.

From X-ray analysis, the bond lengths of C=C and C=O of a CHL molecule in MTDTPY-CHL are larger than those of a neutral CHL. These values are close to those in TMPD (*N,N,N',N'*-tetramethyl-1,4-phenylenediamine)-CHL with a degree of CT of ca. 0.6.[6] Figure 11 shows the energy band structure of MTDTPY-CHL, assuming that the degree of CT is 0.6. The energy bands for MTDTPY and CHL show a one-dimensional character with a strong dispersion along the stacking direction. They cross each other and the band gaps come out at the crossing points. This manner is in contrast with the parallel bands in

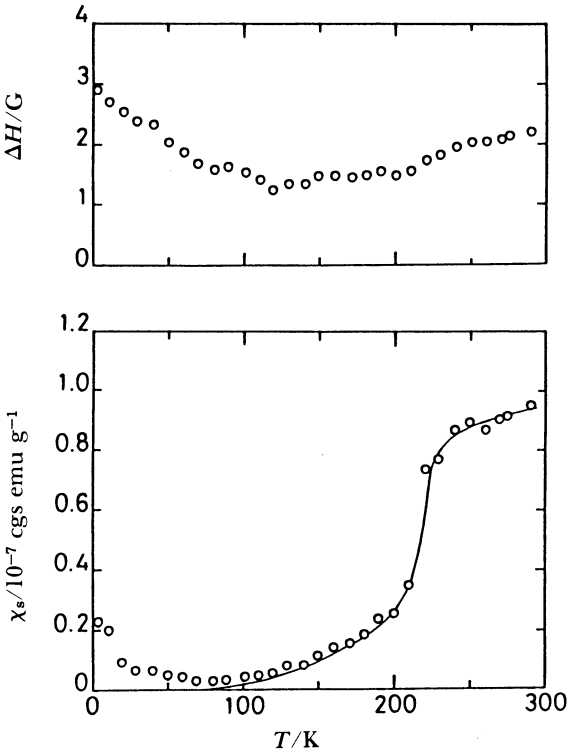

Fig. 10. Temperature dependence of the linewidth (ΔH) and the spin susceptibility (χ_s) for MTDTPY-chloranil. The solid line is obtained after a subtraction of the Curie tail at low-temperatures.

β-MTDTPY-TCNQ. The band structure is semimetallic with electron and hole carriers at the Fermi energy. Accordingly, electron and hole pockets coexist at the Fermi surface in the Brillouin zone.

Next, we present the results concerning the electrical property of MTDTPY-BRL. As shown in Fig. 7, MTDTPY-BRL has a metallic character down to 125 K. The resistivity at room temperature is 4.3×10^{-3} Ωcm, which is lower than 7.0×10^{-3} Ωcm of MTDTPY-CHL. The resistivity decreases gradually down to 175 K and shows a broad minimum, and then increases gradually. Thereafter, the resistivity increases sharply below 125 K, which suggests the occurrence of a metal-insulator transition. This transition temperature is lower compared with 240 K of MTDTPY-CHL. MTDTPY-BRL does not show any hysteresis in the resistivity, dissimilar to MTDTPY-CHL.

Discussion

β-MTDTPY-TCNQ. In a β-MTDTPY-TCNQ crystal, MTDTPY and TCNQ molecules are segregately stacked to form uniform columns along the c-axis with interplanar spacings of 3.48 Å for MTDTPY stacks and 3.27 Å for TCNQ stacks.[6] The degree of CT was evaluated to be 0.6—0.7 from the CN stretching frequency and the bond length in a TCNQ molecule. Such a segregated stack structure and partial CT, which are favorable for realizing organic metals, give a

Table 2. Overlap Integrals of the HOMO, the LUMO, and the HOMO-LUMO in MTDTPY-Chloranil

Molecules	Crystal direction[a)]	Overlap integral $\times10^{-3}$
MTDTPY-MTDTPY	c	−6.81
MTDTPY-MTDTPY	a+b+c	−1.01
MTDTPY-MTDTPY	a+b	−0.32
CHL-CHL	c	10.35
CHL-CHL	a+b	−0.23
MTDTPY-CHL	a/2+b+c	0.15

a) The definition of the crystal axes is described in Ref. 6.

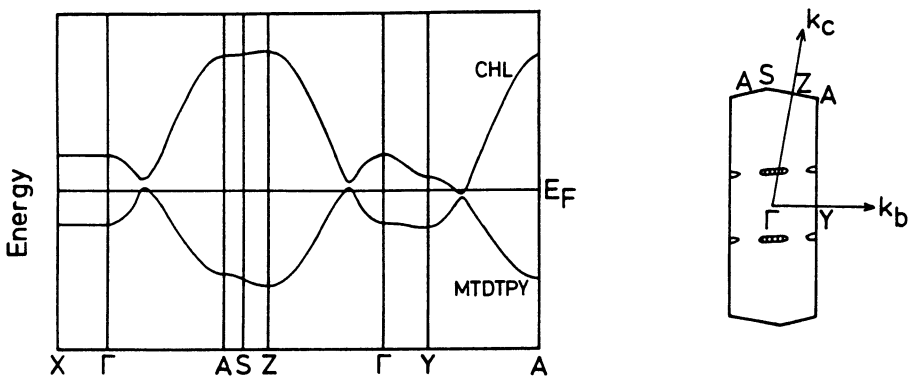

Fig. 11. Energy band structure and Fermi surface of MTDTPY-chloranil. The shaded and non-shaded regions indicate the hole and electron parts, respectively.

metallic conductivity. β-MTDTPY-TCNQ has a two-chain conducting system due to a partial CT from MTDTPY to TCNQ. A thermoelectric power measurement is useful for determining which carrier is dominant in electrical conduction. The negative thermoelectric power at high-temperature means that the electron carriers on TCNQ columns predominate in electrical conduction. The shift of its sign below 150 K implies that the sort of carriers which play the main role of electrical conduction changes from electron carriers on TCNQ columns to hole carriers on MTDTPY columns. The change of the main conduction path affects the electronic properties, since the resistivity starts to increase steeply below 150 K.

A band calculation presents a one-dimensional electronic structure with large anisotropy of the transfer integral between MTDTPY molecules and between TCNQ molecules, and weak intermolecular interaction between MTDTPY and TCNQ molecules. The sharp ESR linewidth of 0.87 G at room temperature is also suggestive of the one-dimensionality of this complex. The linewidth with the Lorentzian line shape can be expressed by the inverse of the spin-lattice relaxation time. The linewidth observed in a one-dimensional metal is extremely narrow, since spin-lattice relaxation through spin-orbit coupling based on the Elliott mechanism is prohibited due to the lack of interchain hopping for pure one-dimensional conductors.[11,12] The spin susceptibility gradually decreases in the metallic region, which deviates from temperature-independent Pauli paramagnetic behavior seen in simple metals. The temperature-dependent Pauli susceptibility has been observed in typical one-dimensional organic metal TTF-TCNQ.[13] The Pauli susceptibility χ_P is related to the density of states at the Fermi energy $N(E_F)$ in the equation $\chi_P=\mu_B{}^2N(E_F)$. For a one-dimensional system, a Peierls gap as a fluctuation already exists in the metallic state and reduces $N(E_F)$. Since the fluctuation is enhanced with lowering temperature, the spin susceptibility shows a decreasing behavior with temperature, even in the metallic region.

β-MTDTPY-TCNQ undergoes an M-I transition around 110 K, judging from an activated behavior in the spin susceptibility χ_s and a decrease proportional to T^{-1} in the thermoelectric power below this temperature. The exponential decrease in χ_s suggests a stabilization of a singlet ground state below T_c. The magnetic activation energy Δ is evaluated to be 0.042 eV with the equation $\chi_s=(C/T)\exp(-\Delta/T)$. This value is in good agreement with E_a of 0.056 eV in the resistivity. The thermoelectric power for intrinsic semiconductors can be approximately expressed in the Boltzmann-transport theory by

$$S = -\frac{k}{|e|}\left(\frac{b-1}{b+1}\cdot\frac{E_a}{kT}+A\right),$$

where b is the mobility ratio μ_e/μ_h between electron and hole carriers, and A is a constant term.[14] The mobility ratio b is calculated to be 2.8 from the slope below 110 K using E_a value of 0.056 eV in the resistivity. This fact means that electron carriers move faster than hole carriers in the semiconductive phase. In the metallic phase, the ESR spectra show a single absorption line due to motional narrowing through interchain coupling between donor and acceptor. Below T_c, the ESR spectra split into two signal components. The splittings of the spectra in the semiconducting phase are attributed to a reduction of the interchain electron hopping rate. The hopping rate is evaluated to be ca. 2×10^{-7} s at 110 K with an absorption line shape simulation for electron hopping model between two sites.[15,16] This rate is quite slow, which means that the interactions between MTDTPY and TCNQ columns are very weak. (The hopping rate for TTF-TCNQ metal is estimated to be 3.7×10^{-12} s from an NMR experiment by Soda et al.[17])

We now discuss the differences in the electronic properties between DTPY-TCNQ and β-MTDTPY-TCNQ. Both complexes possess segregated stacks of donor and acceptor molecules in their crystals. The significant difference is the manner of interatomic contact between an S atom in a donor molecule and an N atom in a TCNQ molecule. DTPY-TCNQ has a contact of 3.40 Å (van der Waals distance: 3.35 Å) between S atom with the high charge density and N atom,[4,5] while β-MTDTPY-TCNQ has a contact of 3.50 Å between the outer S atom with the low charge density and N atom.[6] According to our band calculation of DTPY-TCNQ, the intermolecular overlap integrals are -3.7×10^{-3} for DTPY stacks, 32.1×10^{-3} for TCNQ stacks, and -6.0×10^{-3} between DTPY and TCNQ stacks. Noticeably, the intermolecular overlapping between DTPY and TCNQ molecules is perceptibly large, which is comparable to that for DTPY stacks and is one-fifth of that for TCNQ stacks. The enhancement of the dimensionality through interchain interactions between DTPY and TCNQ stacks is considered to suppress the Peierls transition in the DTPY-TCNQ system. In the case of β-MTDTPY-TCNQ, the intermolecular interaction between MTDTPY and TCNQ stacks is very weak with a minute overlap integral. The marked one-dimensionality may give rise to the Peierls transition at a higher temperature.

MTDTPY-CHL. The electronic property in the metallic state of MTDTPY-CHL closely resembles that of β-MTDTPY-TCNQ. According to an X-ray diffraction study, the MTDTPY-CHL crystal possesses a uniform segregated stack structure with interplanar distances of 3.47 Å for MTDTPY stacks and 3.22 Å for CHL stacks.[6] The bond lengths of CHL in MTDTPY-CHL complex suggest a partial CT state. These facts realize a metallic conduction in this complex. A theoretical calculation exhibits the semimetal-

lic band structure with electron and hole carriers. The positive thermoelectric power of 20 $\mu V K^{-1}$ at room temperature tells that the electrical conduction is dominated by hole carriers. The one-dimensional nature of this complex is shown in the narrow ESR linewidth of 2.2 G at room temperature, the large $t_{\parallel}/t_{\perp}$ for both MTDTPY and CHL stacks and the weak interchain interaction between MTDTPY and CHL stacks. Hence, the Pauli susceptibility depends on the temperature, even in the metallic state, due to a one-dimensional fluctuation.

MTDTPY-CHL is considered to have a Peierls transition at 240 K, since below this temperature the resistivity increases abruptly and the thermoelectric power increases proportionally to T^{-1} and the spin susceptibility decreases in an activated manner with Δ=0.091 eV. Characteristically, MTDTPY-CHL shows a first-order phase transition with the hysteresis in the resistivity and the thermoelectric power around 110 K, which suggests the presence of some transformation in the crystal structure. This first-order phase transition is smeared out upon applying pressure above ca. 5 kbar.

Finally, we briefly mention of the relation between the conductivity and the ionicity of the complex. The ionicity of the complex is mainly goverened by the difference (I_p—E_A) between an ionization energy I_p of a donor and an electron affinity E_A of an acceptor. A small (I_p—E_A) gives an ionic complex, while a large one gives a neutral complex. A complex with a partial CT is realized under the condition (I_p—E_A)≈E_M (E_M: crystal Madelung energy).[18] As to *p*-benzoquinone derivatives used in this work, the ability of an acceptor increases in BRL≈CHL≪DDQ. MTDTPY-BRL and MTDTPY-CHL show high conductivities owing to a partial CT of ca. 0.6. MTDTPY-DDQ shows the highest resistivity, 5.4 Ωcm, since the ionicty of the complex approaches the ionic state with a decrease of (I_p—E_A).

Summary

α-MTDTPY-TCNQ, MTDTPY-FLL, and MTDTPY-DDQ are semiconductors, whereas β-MTDTPY-TCNQ, MTDTPY-CHL, and MTDTPY-BRL show metallic conductivity. X-Ray diffraction studies confirm that metallic conductions in β-MTDTPY-TCNQ and MTDTPY-CHL are owing to uniform segregated stacks and a partial charge-transfer state. MTDTPY-CHL and MTDTPY-BRL are the first organic metals among the *p*-benzoquinone derivatives complexes ever known. Theoretical calculations give one-dimensional electronic structures for β-MTDTPY-TCNQ and MTDTPY-CHL. ESR measurements also suggest one-dimensionality with a narrow linewidth and temperature-dependent Pauli susceptibility. Thus, the origin of the metal-insulator (M-I) transitions at 110 and 240 K for β-MTDTPY-TCNQ and MTDTPY-CHL, respectively, can be attributed to a Peierls instability. These complexes show novel behaviors in the semiconducting region. In the case of β-MTDTPY-TCNQ, the ESR spectra are separated into two components below T_{MI}. The splittings of the spectra can be explained by a slow interchain hopping rate of electrons between MTDTPY and TCNQ molecules. MTDTPY-CHL has a first-order phase transition around 110 K. This phase transition is easily suppressed by pressure above ca. 5 kbar. MTDTPY-BRL, without a first-order phase transition, shows a lower M-I transition temperature of 125 K.

β-MTDTPY-TCNQ and MTDTPY-CHL have two-dimensional networks in the crystals through interchain S-S contacts less than the van der Waals distance.[6] However, their electronic properties are one-dimensional, as presented in the results of ESR and band calculation. The selection of the other acceptors or another chemical modifications will be needed to achieve an intention for enhancing the dimensionality to stabilize a metallic state.

The authors are grateful to Dr. Shunji Bandow of Institute for Molecular Science for his helpful support in the ESR simulation.

References

1) H. Akamatu, H. Inokuchi, and Y. Matsunaga, *Nature (London)*, **173**, 168 (1954).

2) H. J. Keller, D. Nöthe, H. Pritzkow, D. Wehe, M. Werner, P. Koch, and D. Schweitzer, *Mol. Cryst. Liq. Cryst.*, **62**, 181 (1980).

3) K. Nakasuji, H. Kubota, T. Kotani, I. Murata, G. Saito, T. Enoki, K. Imaeda, H. Inokuchi, M. Honda, C. Katayama, and J. Tanaka, *J. Am. Chem. Soc.*, **108**, 3460 (1986).

4) N. Thorup, G. Rindorf, C. S. Jacobsen, K. Bechgaard, I. Johannsen, and K. Mortensen, *Mol. Cryst. Liq. Cryst.*, **120**, 349 (1985).

5) K. Bechgaard, *Mol. Cryst. Liq. Cryst.*, **125**, 81 (1985).

6) K. Nakasuji, M. Sasaki, T. Kotani, I. Murata, T. Enoki, K. Imaeda, H. Inokuchi, A. Kawamoto, and J. Tanaka, *J. Am. Chem. Soc.*, **109**, 6970 (1987).

7) P. M. Chaikin and J. F. Kwak, *Rev. Sci. Instrum.*, **46**, 218 (1975).

8) T. Mori, A. Kobayashi, Y. Sasaki, H. Kobayashi, G. Saito, and H. Inokuchi, *Bull. Chem. Soc. Jpn.*, **57**, 627 (1984).

9) T. Mori, Ph. D Thesis, The University of Tokyo, Tokyo, Japan (1985).

10) M. Kinoshita and H. Akamatu, *Nature (London)*, **207**, 291 (1965).

11) R. J. Elliott, *Phys. Rev.*, **96**, 266 (1954).

12) Y. Tomkiewicz, E. M. Engler, and T. D. Schultz, *Phys. Rev. Lett.*, **35**, 456 (1975).

13) Y. Tomkiewicz, A. R. Taranko, and J. B. Torrance, *Phys. Rev. B*, **15**, 1017 (1977).

14) P. M. Chaikin, R. L. Greene, S. Etemad, and E. Engler, *Phys. Rev. B*, **13**, 1627 (1976).

15) K. Kuwata and G. Soda, "Kanwagenshō No Kagaku,"

ed by K. Higashi and S. Nagakura, Iwanami, Tokyo (1973), Chap. 2.
16) A. Carrington and A. D. McLachlan, "Introduction to Magnetic Resonance," Chapman and Hall, London (1979), Chap. 12.
17) G. Soda, D. Jerome, M. Weger, J. M. Fabre, and L. Giral, *Solid State Commun.*, **18**, 1417 (1976).
18) J. B. Torrance, J. E. Vazquez, J. J. Mayerle, and V. Y. Lee, *Phys. Rev. Lett.*, **46**, 253 (1981).